AD-A116 950 BOSTON COLL CHESTNUT HILL MA DEPT OF PHYSICS F/G 20/3
PARTICLE TRAJECTORIES IN A MODEL ELECTRIC FIELD II,(U)
DEC 81 P CARINI, G KALMAN, Y SHIMA F19628-79-C-0031
UNCLASSIFIED SCIENTIFIC-2 AFGL-TR-82-0149 NL

END
DATE FILMED
8-82
DTIC

AD A116950

AFGL-TR-82-0149

PARTICLE TRAJECTORIES IN A MODEL ELECTRIC FIELD II

Paul Carini
Gabor Kalman
Yaakov Shima

Boston College
Department of Physics
Chestnut Hill, Ma 02167

Scientific Report No. 2

15 December 1981

AIR FORCE GEOPHYSICS LABORATORY
AIR FORCE SYSTEMS COMMAND
UNITED STATES AIR FORCE
HANSCOM AFB, MASSACHUSETTS 01731

Unclassified

SECURITY CLASSIFICATION OF THIS PAGE (When Data Entered)

REPORT DOCUMENTATION PAGE		READ INSTRUCTIONS BEFORE COMPLETING FORM
1. REPORT NUMBER AFGL-TR-82-0149	2. GOVT ACCESSION NO. AD A116950	3. RECIPIENT'S CATALOG NUMBER
4. TITLE (and Subtitle) PARTICLE TRAJECTORIES IN A MODEL ELECTRIC FIELD II		5. TYPE OF REPORT & PERIOD COVERED Scientific Report No. 2
		6. PERFORMING ORG. REPORT NUMBER
7. AUTHOR(s) Paul Carini Gabor Kalman Yaakov Shima		8. CONTRACT OR GRANT NUMBER(s) F19628-79-C-0031
9. PERFORMING ORGANIZATION NAME AND ADDRESS Boston College Department of Physics Chestnut Hill, MA 02167		10. PROGRAM ELEMENT, PROJECT, TASK AREA & WORK UNIT NUMBERS 62101F 766106AJ
11. CONTROLLING OFFICE NAME AND ADDRESS Air Force Geophysics Laboratory Hanscom AFB, Massachusetts 01731 Monitor/David A. Hardy, Lt. USAF/PHG		12. REPORT DATE 15 December 1981 13. NUMBER OF PAGES 27
14. MONITORING AGENCY NAME & ADDRESS(if different from Controlling Office)		15. SECURITY CLASS. (of this report) Unclassified 15a. DECLASSIFICATION/DOWNGRADING SCHEDULE

16. DISTRIBUTION STATEMENT (of this Report)

Approved for public release; distribution unlimited

17. DISTRIBUTION STATEMENT (of the abstract entered in Block 20, if different from Report)

18. SUPPLEMENTARY NOTES

19. KEY WORDS (Continue on reverse side if necessary and identify by block number)

Spacecraft Charging
Electric Fields
Particle Trajectories

20. ABSTRACT (Continue on reverse side if necessary and identify by block number)

The report examines the feasibility of neutralizing the potential difference that occurs on a spacecraft by emitting ions from the positively charged surface region of the spacecraft and lefting this current impact on the negatively charged surface region. The investigation was performed by making two different simplifying assumptions about the geometry of the problem. In the first case we approximated the geometry by two conducting infinite half planes. In the second case we approximated the geometry by two finite width constant charge density plates. In both cases we investigated

DD FORM 1 JAN 73 1473 EDITION OF 1 NOV 65 IS OBSOLETE

Unclassified

SECURITY CLASSIFICATION OF THIS PAGE (When Data Entered)

the dependence of the particle trajectories on the origination, velocity, and direction of emission of the particles. Two generalizations emerge from the study: 1) Shallow launch angles give more favorable trajectories. 2) For a given launch angle there is an optimum energy which yields a minimum impact distance.

Abstract

The report examines the feasibility of neutralizing the potential difference that occurs on a spacecraft by emitting ions from the positively charged surface region of the spacecraft and lefting this current impact on the negatively charged surface region. The investigation was performed by making two different simplifying assumptions about the geometry of the problem. In the first case we approximated the geometry by two conducting infinite half planes. In the second case we approximated the geometry by two finite width constant charge density plates. In both cases we investigated the dependence of the particle trajectories on the origination, velocity, and direction of emission of the particles. Two generalizations emerge from the study: 1) Shallow launch angles give more favorable trajectories. 2) For a given launch angle there is an optimum energy which yields a minimum impact distance.

I. INTRODUCTION

The investigation completed for this report studied the feasibility of neutralizing the potential difference which occurs on the surface of a spacecraft. It has been proposed that neutralization can be accomplished by emitting ions from the positively charged surface region of the spacecraft and by letting this current impact on the negatively charged surface region. In order to investigate the main features of the proposed scheme we made some simplifying assumptions about the geometry of the problem. In the first case we approximated the geometry by two conducting infinite half planes and investigated the trajectories of a positive ion emitted at some point on the positively charged half plane with given initial velocity and given direction of emission.

In the second case we approximated the geometry by two constant charge density finite width strips and investigated the trajectories of a positive ion emitted at some point on the positively charged strip with respect to origination, velocity and direction. The second case probably provides a more realistic description of actual satellite conditions.

II. POTENTIAL DUE TO TWO CONDUCTING INFINITE HALF PLANES

A. Statement of problem

This case was already discussed in Scientific Report #1. We provide here a review of the problem along with more complete solutions and conclusions.

We consider the plane $y=o$ and assume a cut on this plane along the z axis. Let there be a given potential difference V between the two half planes $x > o$ and $x < o$. The equations of motion of a charged particle in the electric field produced in such a configuration are

$$m\frac{d^2x}{dt^2} = \frac{-eV}{\pi}\frac{y}{x^2+y^2}$$

$$m\frac{d^2y}{dt^2} = \frac{eV}{\pi}\frac{x}{x^2+y^2}$$

$$m\frac{d^2z}{dt^2} = o$$

Motion in the z direction is trivial and not related to the problem. The remaining equations can be cast in a dimensionless form

$$\frac{d^2x}{dt^2} = \frac{-y}{x^2+y^2}$$

$$\frac{d^2y}{dt^2} = \frac{x}{x^2+y^2}$$

with the initial conditions that at time t=o

$$x = 1 \qquad v_y = v_{xo}$$

$$y = o \qquad v_y = v_{yo}$$

and where the initial velocities v_{xo} and v_{yo} are in units of $\sqrt{\frac{eV}{m\pi}}$.

B. Numerical Solution

Since no analytical solutions to the above equations could be found they were solved numerically using a modified version of scientific subroutine DHPCG based on Hamming's Modified Predictor Corrector Method. Table 1 lists the values of x_* (the impact distance) for various values of $v_T = \sqrt{v_x^2+v_y^2}$ (the total initial velocity) and the initial launch angle θ. Table 2 lists the values of Y_{max} (the maximum height attained by the first particle for various values of $v_T = \sqrt{v_x^2+v_y^2}$ and the initial launch angle. Data for the blank areas of both tables were not obtainable in a reasonable amount of computer iterations due to their large size.

The discrepencies between these results and the earlier ones given in the previous report for larger values of v_t are due to defects in the earlier computer program. Figure 1 shows the dependence of x_* (the impact distance) on v_t (the total initial velocity) and θ (the launch angle). Figure 2 shows the dependence of y_{max} (the maximum height) on v_t (the total initial velocity) and θ (the launch angle). The figures show that both x_* and y_{max} have a similar dependence on v_t and θ. Note also that for a given launch angle (except: $\theta = 0$) both x_* and y_{max} have a minimum for some v_t in the range $0 \leq v_t \leq 2$ (in units of $\sqrt{\frac{eV}{m\pi}}$).

C. Asymptotic Result

As can be seen in figure 1 for 0^o launch angle the impact distance x_* tends to 0 for large initial velocities. This can be demonstrated analytically by approximating the basic equations

$$\ddot{x} = \frac{-y}{x^2+y^2}$$

$$\ddot{y} = \frac{x}{x^2+y^2}$$

For large initial velocity v_{xo} and 0^o launch angle the trajectory height, x_*, is expected to remain close to zero. Approximating $y = 0$ in the above equations leads to

$$\ddot{x} = 0 \quad \text{which yields} \quad x = 1 + v_{xo}t$$

$$\ddot{y} = \frac{1}{1+v_{xo}t}$$

This equation may be integrated immediately and thus gives for $\dot{y}$

$$\dot{y} = \frac{1}{v_{xo}} \ln(1+v_{xo}t).$$

The equation for y may be obtained by integrating again

$$y = \frac{1}{v_{xo}^2}\left[(1+v_{xo}t)\ln(1+v_{xo}t) - (1+v_{xo}t)+1\right]$$

To find the impact distance x_*, we set y=o and substitute for $x = 1+v_{xo}t$

$$0 = x\ln x - x + 1$$

or $$\ln x = 1 - \frac{1}{x}$$

To find solutions for negative x we can rewrite the equation as

$$\ln x = 1 + \frac{1}{x}$$

and solve for positive x.

This yields x = 3.59112 as a solution.

Therefore we see that the launch angle $\theta=0^\circ$ curve in figure 1 has as an asymptote the line x=3.59 in the limit of large initial velocity. This impact distance $x_* = 3.59$ would be the shortest obtainable impact distance under the most favorable conditions in this geometrical approximation. The data in Table 1 verify this conclusion.

III. POTENTIAL DUE TO FINITE WIDTH CONSTANT CHARGE DENSITY PLATES

A. Statement of the Problem

We consider the plane y=0 and assume a cut on this plane along the Z axis. Let there be a constant charge desnity in the two infinite length strips $-a<x<o$ and $o<x<a$. One can calculate the potential, v_1 for this geometry by starting with the potential for a line charge and integrating over the area of the strips with the result

$$v = \frac{-V}{\pi} \left\{ x \ln \left[\frac{[(x-a)^2+y^2][(x+a)^2+y^2]}{(x^2+y^2)^2} \right] + a \ln \left[\frac{(x+a)^2 + y^2}{(x-a)^2+y^2} \right] \right.$$

$$\left. + 2y \left[\tan^{-1} \left(\frac{x-a}{y}\right) + \tan^{-1} \left(\frac{x+a}{y}\right) - 2 \tan^{-1} \left(\frac{x}{y}\right) \right] \right\}$$

The electric field follows directly from the potential.

$$E_x = \frac{V}{\pi} \left[\ln \frac{[(x-a)^2+y^2][(x+a)^2+y^2]}{(x^2+y^2)^2} \right]$$

$$E_y = \frac{V}{\pi} 2 \left\{ \tan^{-1} \left(\frac{x-a}{y}\right) + \tan^{-1} \left(\frac{x+a}{y}\right) - 2 \tan^{-1} \left(\frac{x}{y}\right) \right\}$$

$$E_z = o$$

The equations of motion are therefore

$$m\ddot{x} = \frac{eV}{\pi} \ln \left\{ \frac{[(x-a)^2+y^2][(x+a)^2+y^2]}{(x^2+y^2)^2} \right\}$$

$$m\ddot{y} = \frac{eV}{\pi} 2 \left\{ \tan^{-1} \left(\frac{x-a}{y}\right) + \tan^{-1} \left(\frac{x+a}{y}\right) - 2 \tan^{-1} \left(\frac{x}{y}\right) \right\}$$

$$m\ddot{0} = o$$

Again motion in the z direction is trivial and not related to the problem. The remaining equations can be case in a dimensionless form

$$\ddot{x} = \ln \left\{ \frac{[(x-a)^2+y^2][(x+a)^2+y^2]}{(x^2+y^2)^2} \right\}$$

$$\ddot{y} = 2 \left\{ \tan^{-1} \left(\frac{x-a}{y}\right) + \tan^{-1} \left(\frac{x+a}{y}\right) - 2 \tan^{-1} \left(\frac{x}{y}\right) \right\}$$

with the initial conditions that at time t=o

$$x = x_o \qquad v_x = v_{xo}$$

$$y = o \qquad v_y = v_{yo}$$

where the initial velocities v_{xo} and v_{yo} are in units of $\sqrt{\frac{eV}{m\pi}}$.

B. Numerical Solution

These equations were solved numerically using a modified version of scientific subroutine DHPCG based on Hamming's Modified Predictor Corrector Method. (For the sake of the numerical calculations we assumed the width of the strips a=10.) Table 3 lists the values of x_* (the impact distance) for various values of $v_t = \sqrt{v_x^2 + v_y^2}$ (the total initial velocity) and θ (the launch angle) with the launch point $x_o = -1$. Table 4 lists the values of y_{max} (the maximum height) for various values of V_t and θ again for $x_o = -1$. Figures 3 and 4 show the variation of the test particle trajectories with different launch positions for $v_t = o$. Note that above $x_o = -7.25$ the trajectories no longer bend to the right and that even for $x_o = -1$ the impact is already beyond the width of the strips (a=10). Figure 5 shows the dependence of the impact distance, x_*, on the total initial velocity V_t and launch angle θ. Figure 6 shows the dependence of the maximum height y_{max} on the total initial velocity V_t and launch angle θ. As in the previous case both x_* and y_{max} have a very similar dependence on these parameters. In this case both x_* and y_{max} have minimums for the total initial velocity in the range $.5 < V_t < 2$ for launch angles below 40^o only. Figures 7, 8, and 9 give a more detailed picture of the dependence of the impact distance and of the maximum height of the trajectory on the parameters. Figure 10 shows the dependence of the impact distance, x_*, and maximum height, y_{max}, on the initial launch position, x_o, for various angles θ. Note that a small increase in x_o can lead to vary large increases in x_* and y_{max}. This dependence was not present in the first case.

IV. CONCLUSIONS

We have examined particle trajectories in two simple electric field configurations. In both cases we found trajectories which struck the target. Two generalizations emerge from this study: 1) shallower launch angles lead to more favorable trajectories and 2) for a given launch angle there is an optimum energy which yields a minimum impact distance. Whether these generalizations remain true in more complicated geometries remains to be investigated.

V. FIGURE CAPTIONS

Figure 1. Conducting plates: plot of impact distance x_* as a function of the total initial velocity v_t for various launch angles θ.

Figure 2. Conducting plates: plot of the maximum height of the trajectory y_{max} as a function of the total initial velocity v_t for various launch angles θ.

Figure 3. Dielectric plates: plot of trajectories as a function of launch position x_o ($v_t = 0$)

Figure 4. Dielectric plates: plot of trajectories as a function of launch position x_o ($v_t = 0$)

Figure 5. Dielectric plates: plot of impact of distance x_* as a function of the total initial velocity v_t for various launch angles θ. (x_o =

Figure 6. Dielectric plates: plot of the maximum height of the trajectory y_{max} as a function of the total initial velocity v_t for various launch angles θ ($x_o = -1$)

Figure 7. Dielectric plates: plots of x_* and y_{max} as functions of the initial horizontal velocity ($x_o = 1$, $\theta = 0$)

Figure 8. Dielectric plates: plots of x_* and y_{max} as functions of the initial vertical velocity ($x_o = 1$, $\theta = 90$)

Figure 9. Dielectric plates: plots of x_* and y_{max} as functions of the launch angle θ ($x_o = 1$, $v_t = 1.0$)

Figure 10. Dielectric plates: plots of x_* and y_{max} as function of the initial launch position x_o for various angles θ. ($v_t = 1.0$)

TABLE 1

Data for x_* (impact distance)

Conducting Plates

v_t	0=o	10	20	30	40	50	60	70	80	90
.1	533	538	550	566	588	617	650	688	731	779
.2	375.1	382.3	400.3	427.9	480.3	522.0	581.8	653.6	738.6	836.8
.4	207.5	220.9	246.3	286.6	365.3	429.6	549.8	695.2	883.9	1119
.6	125.4	141.5	172.4	224.3	303.4	427.6	608.0	859.6	1227	1729
.8	83.47	100.2	154.1	197.4	302.4	479.7	770.8	1227	1935	
1.0	58.47	76.4	114.9	194.5	339.1	611.8	1114	1921		
2	18.63	46.6	153.0	556.6						
3	10.74	70.4	650.8	1087						
4	7.76	186.3								
5	6.28	764.9								
6	5.54	2609.								
7	4.95									
8	4.81									
9	4.56									
10	4.43									
20	3.85									
40	3.66									

TABLE 2

Conducting Plates — Data for y_{max}

v_t	$\theta = 0$	10	20	30	40	50	60	70	80	90
.1	34.6	34.9	35.6	36.6	38.1	39.9	42.1	44.5	47.3	50.3
.2	24.23	24.71	25.83	27.58	30.96	33.66	37.50	42.12	47.51	53.79
.4	13.27	14.07	15.70	18.21	23.10	27.14	34.54	43.66	55.46	69.98
.6	7.81	8.77	10.67	13.79	18.54	25.96	36.76	52.52	73.98	104.0
.8	5.02	6.01	7.98	11.61	17.67	27.79	44.27	70.32	110.8	
1.0	3.35	4.37	6.49	10.77	18.65	33.35	60.33	103.6		
2	.78	1.88	5.88	20.80	83.86					
3	.31	1.85	16.08	30.52						
4	.16	3.21								
5	.098	9.13								
6	.065	26.81								
7	.046									
8	.035									
9	.027									
10	.022									
20	.00515									
40	.00125									

TABLE 3

Dielectric Plates — Data for x_* (impact distance)

v_t	θ=0	10	20	30	40	50	60	70	80	90
0	10.82									
.1	10.54	10.53	10.52	10.83	10.85	10.87	10.89	11.15	11.17	11.19
.2	10.24	10.27	10.41	10.58	10.93	11.23	11.27	11.52	11.57	11.67
.4	9.68	10.06	10.20	10.53	11.05	11.35	11.83	12.31	12.59	12.88
.6	9.05	9.86	9.97	10.48	11.16	11.81	12.43	13.41	13.82	14.41
.8	8.85	9.19	9.95	10.63	11.66	12.26	13.21	14.49	15.39	16.10
1.0	8.16	8.97	9.92	10.78	11.77	13.09	14.17	15.57	17.11	18.94
2	6.82	8.10	9.70	11.70	14.28	17.59	22.10	28.06	36.03	46.40
4	4.66	7.82	11.31	17.18	30.10	76.09				
6	3.69	8.82	15.64	42.96						
∞	3.24	10.32	31.07							
10	3.07	13.11								

TABLE 4

Dielectric Plates — Data for y_{max}

v_t	$\theta = 0$	10	20	30	40	50	60	70	80	90
0	1.30									
.1	1.24	1.26	1.27	1.299	1.316	1.33	1.35	1.37	1.39	1.40
.2	1.18	1.21	1.25	1.294	1.319	1.37	1.40	1.44	1.47	1.50
.4	1.07	1.14	1.21	1.286	1.33	1.44	1.51	1.59	1.65	1.71
.6	.98	1.07	1.17	1.282	1.36	1.51	1.63	1.75	1.85	1.94
.8	.89	1.01	1.14	1.285	1.39	1.59	1.76	1.91	2.06	2.20
1.0	.81	.95	1.11	1.292	1.43	1.68	1.89	2.10	2.29	2.47
2	.52	.76	1.04	1.386	1.48	2.22	2.70	3.23	3.78	4.34
4	.25	.60	1.11	1.803	1.77	4.18	6.90			
6	.13	.58	1.34	2.524	2.71					
8	.086	.63	1.70							
10	.058	.71								

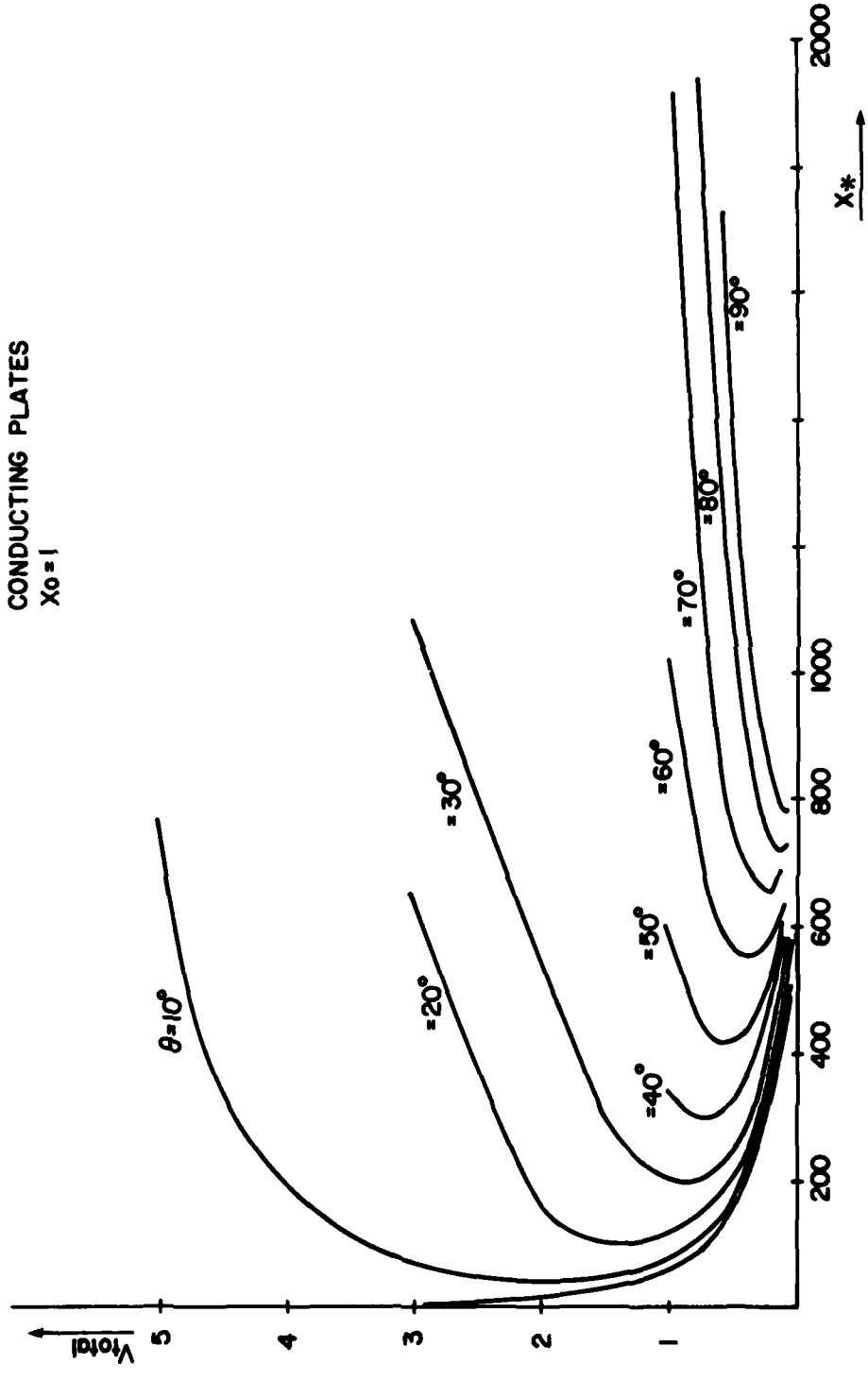
CONDUCTING PLATES
X₀=1
θ=10°
=20°
=30°
=40°
=50°
=60°
=70°
=80°
=90°
V/total
X*
1
2
3
4
5
200
400
600
800
1000
2000

FIG. 1

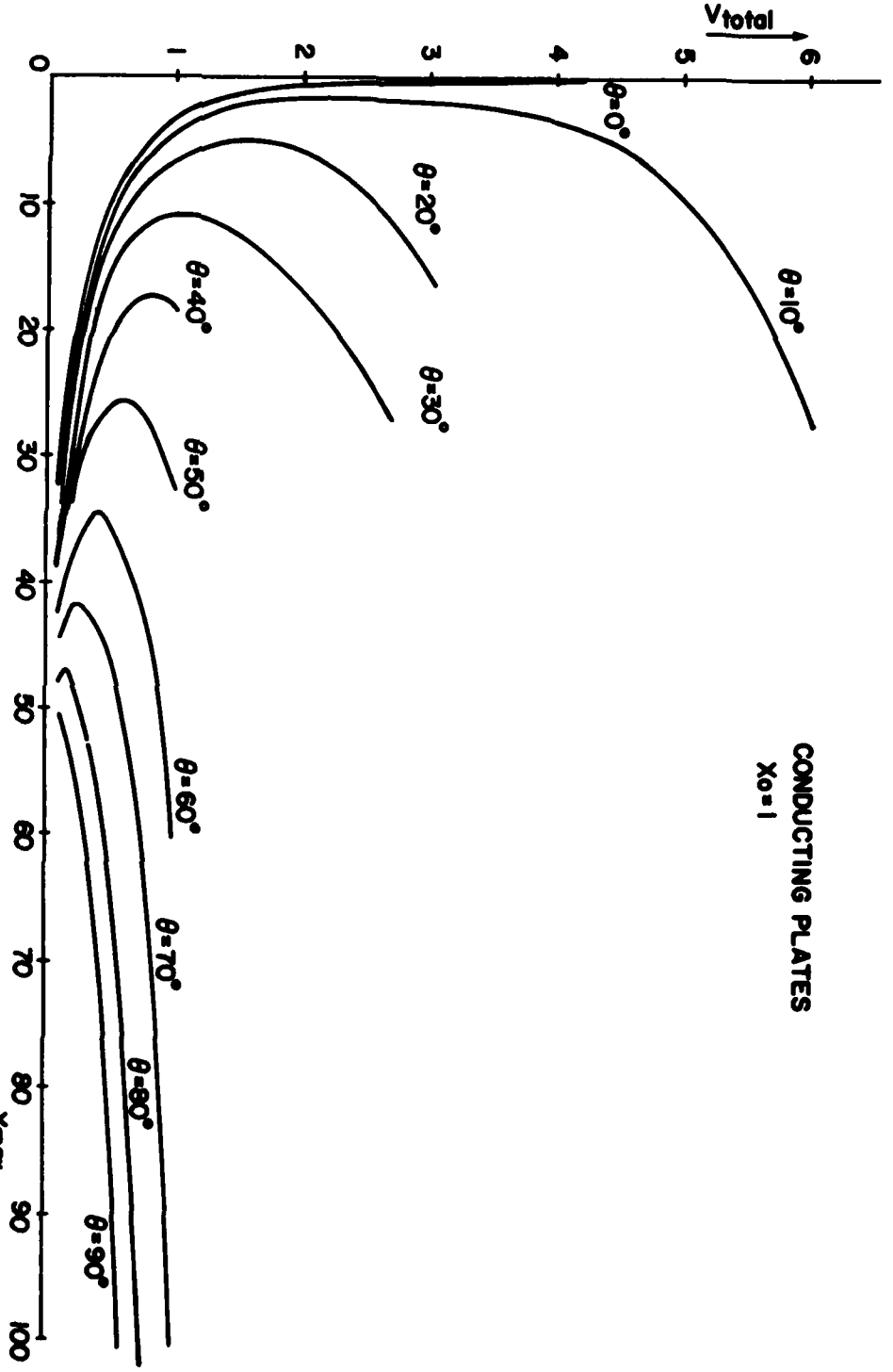
Vtotal
0
1
2
3
4
5
6
θ=0°
θ=10°
θ=20°
θ=30°
θ=40°
θ=50°
θ=60°
θ=70°
θ=80°
θ=90°
Ymax
10
20
30
40
50
60
70
80
90
100
CONDUCTING PLATES
Xo=1

FIG. 2

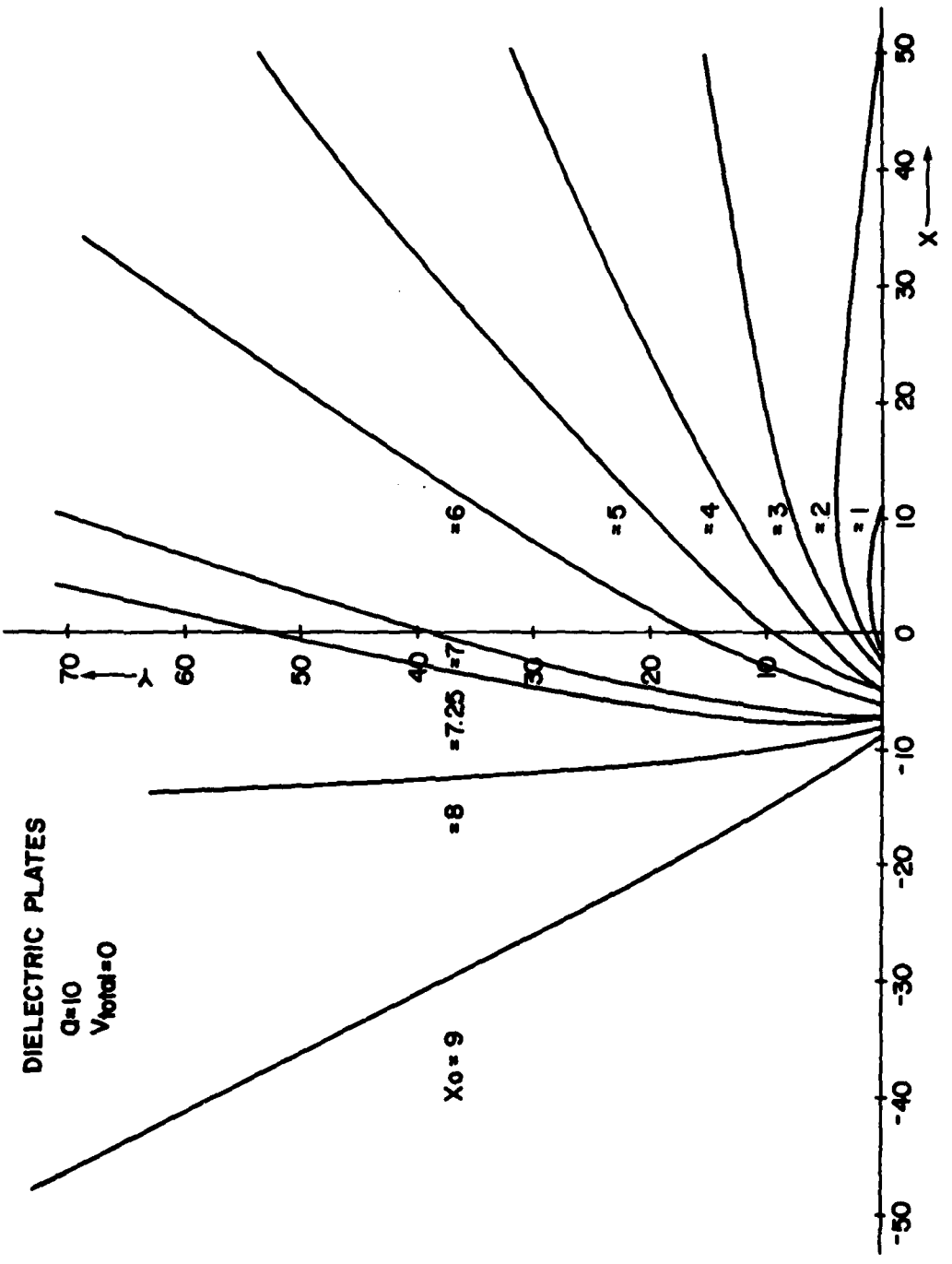
DIELECTRIC PLATES
a=10
V total=0
Xo=9
=8
=7.25
=7
=6
=5
=4
=3
=2
=1
Y
X
70
60
50
40
30
20
10
0
-10
-20
-30
-40
-50
10
20
30
40
50

FIG. 3

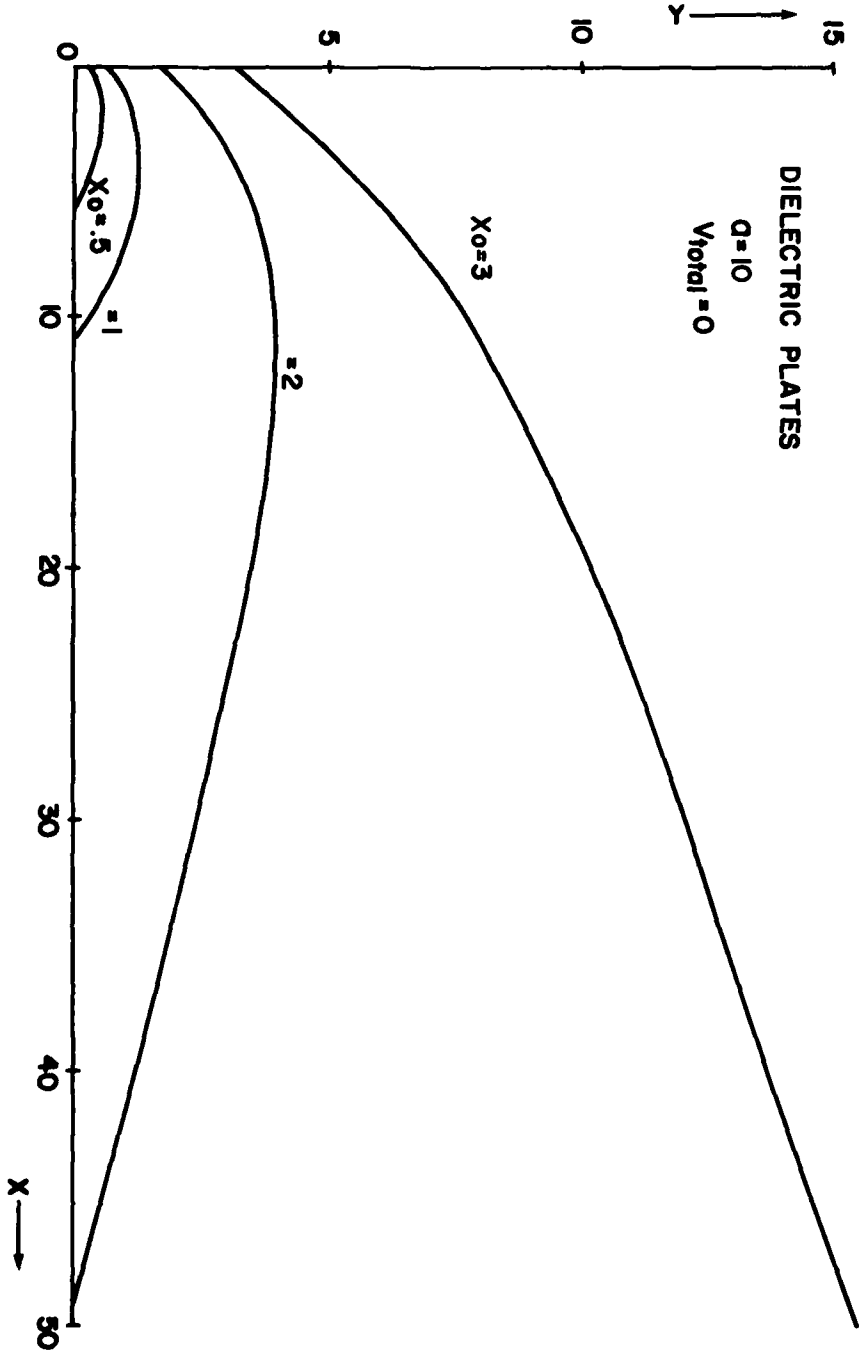
Y
0
5
10
15
X
10
20
30
40
50
DIELECTRIC PLATES
Q=10
Vtotal=0
Xo=.5
=1
=2
Xo=3

FIG. 4

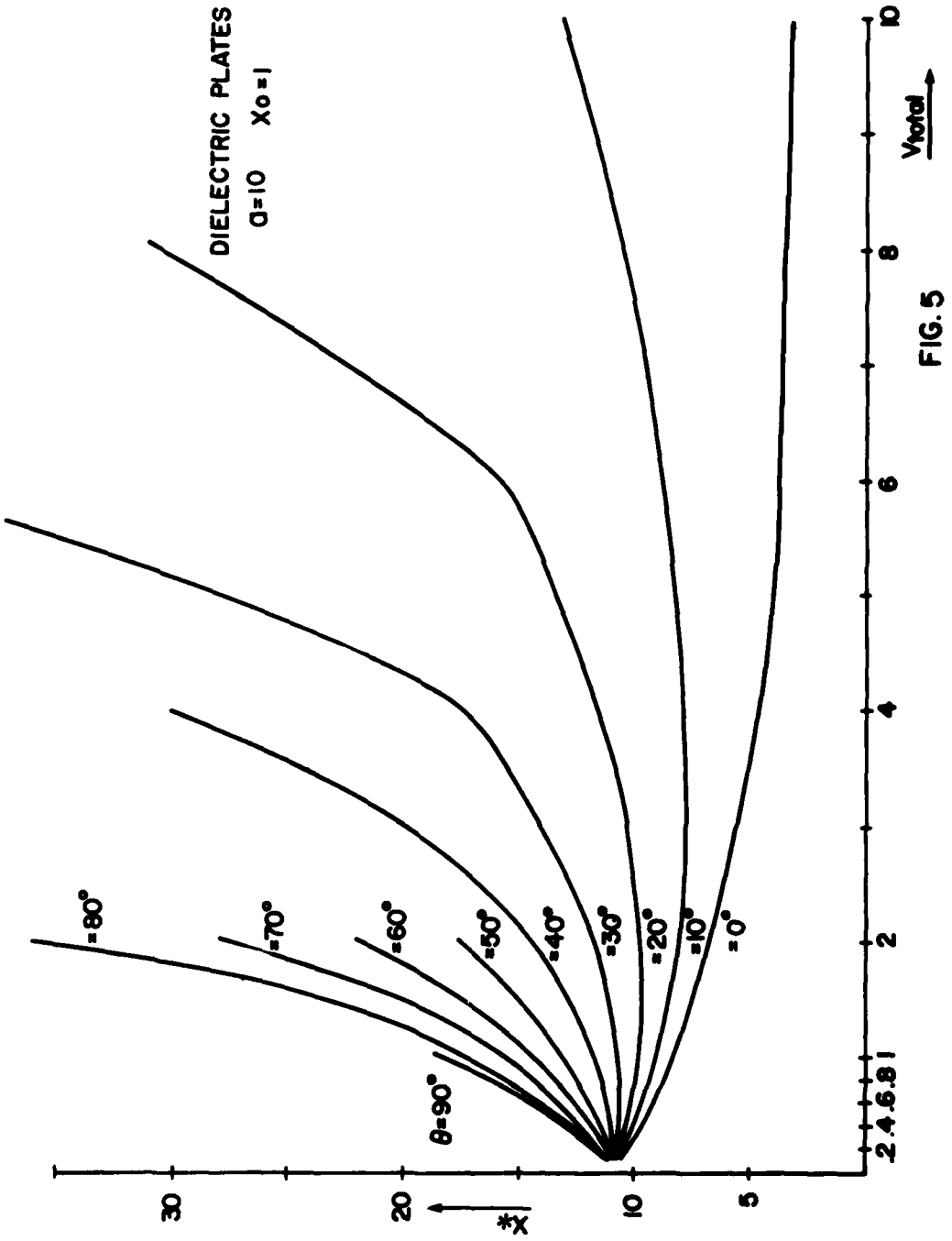
DIELECTRIC PLATES
Q=10 Xo=1
θ=90°
=80°
=70°
=60°
=50°
=40°
=30°
=20°
=10°
=0°
30
20
10
5
X
2.4.6.8.1
2
4
6
8
10
Vtotal

FIG. 5

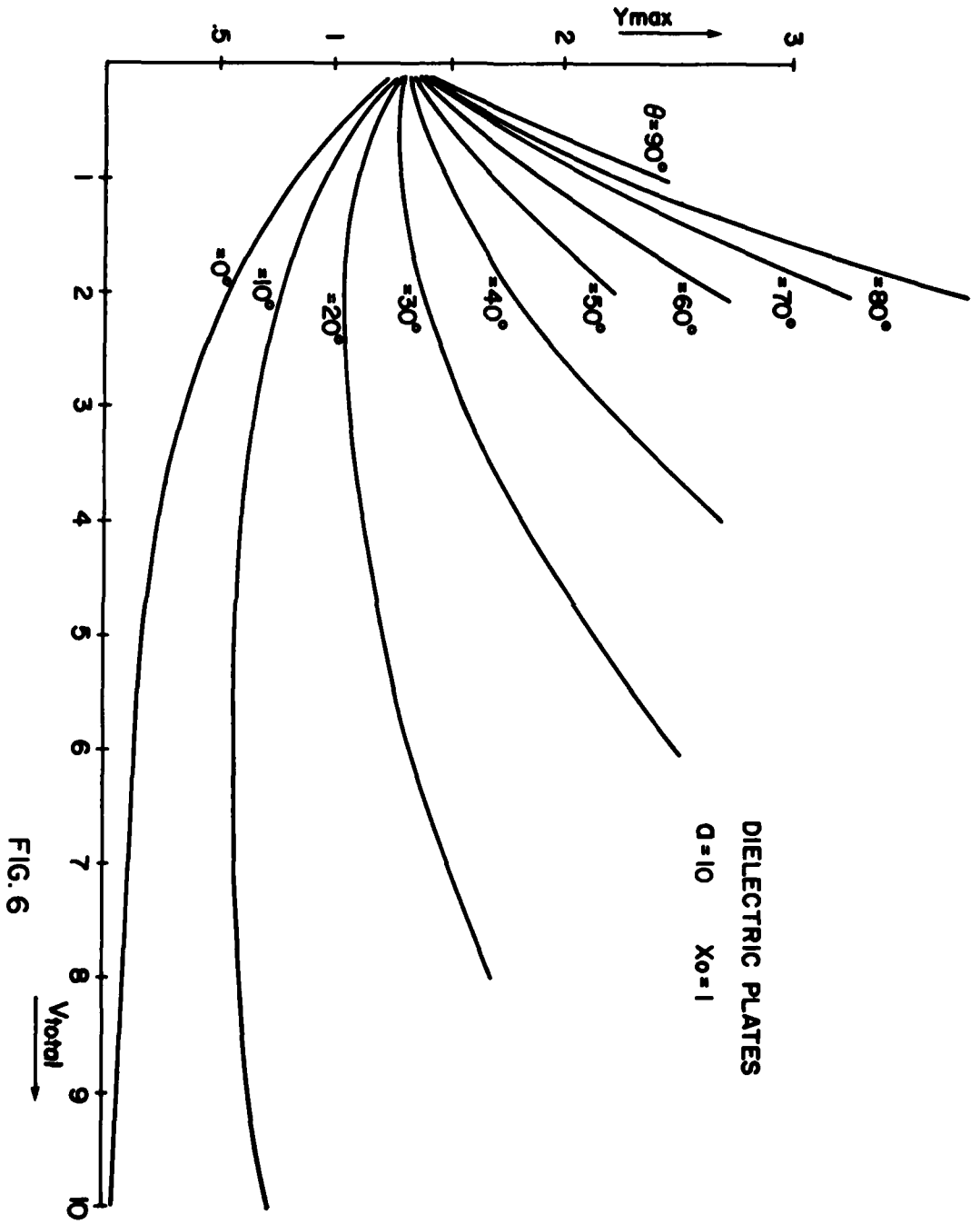
Ymax
.5
1
2
3
θ=90°
=80°
=70°
=60°
=50°
=40°
=30°
=20°
=10°
=0°
1
2
3
4
5
6
7
8
9
10
Vtotal
DIELECTRIC PLATES
a=10 Xo=1

FIG. 6

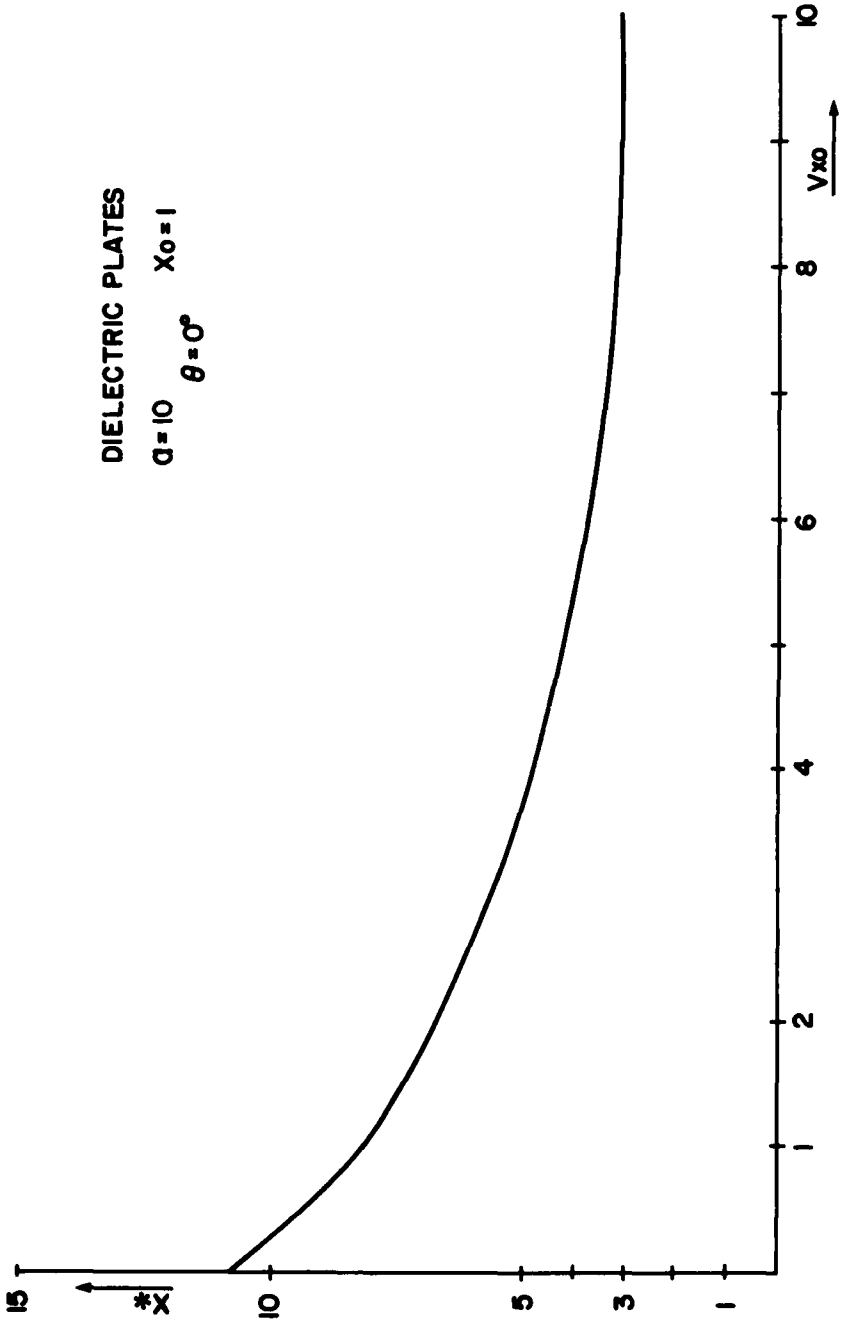

FIG. 7a

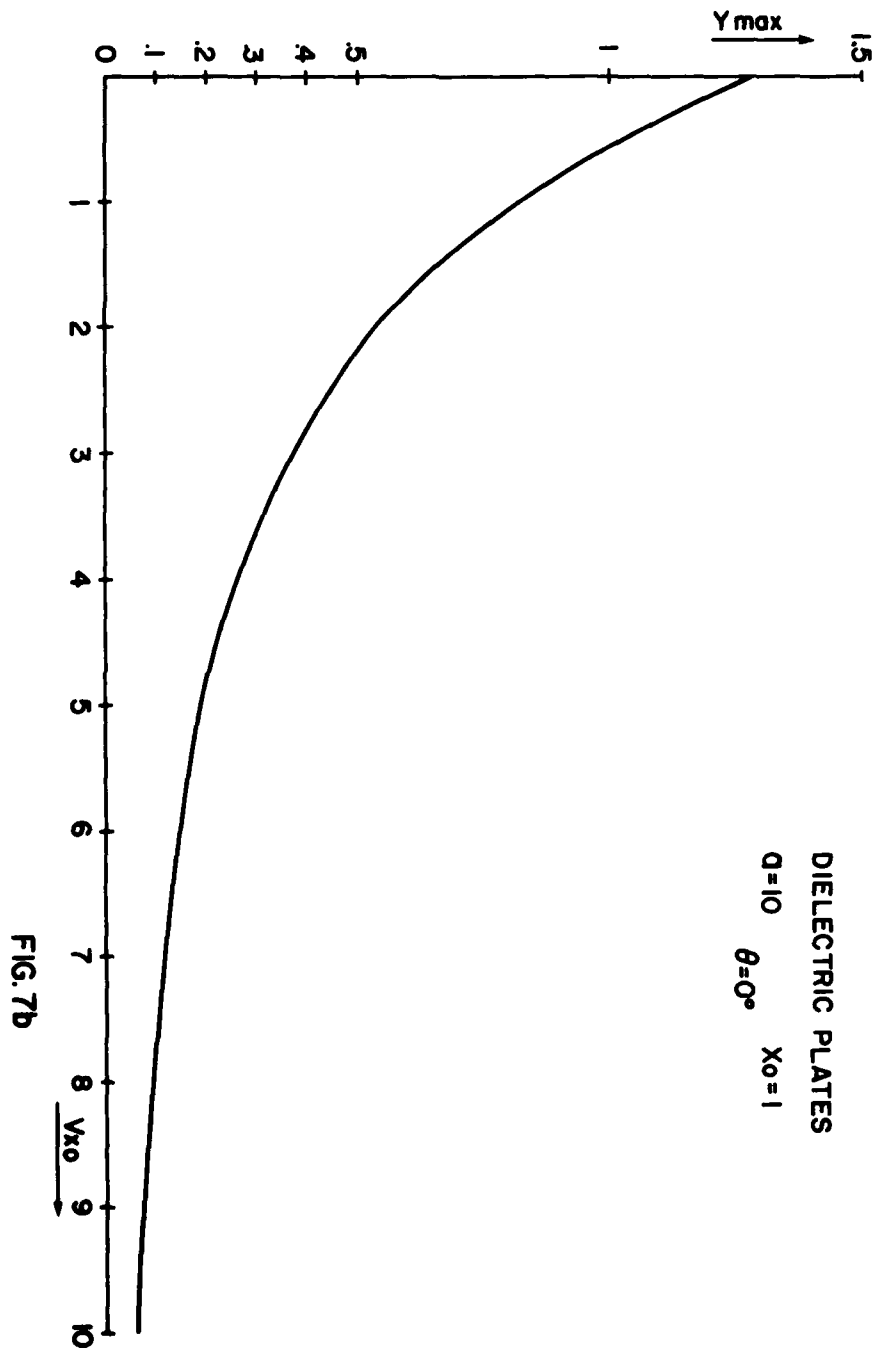
Ymax
0
.1
.2
.3
.4
.5
1
1.5
1
2
3
4
5
6
7
8
9
10
Vxo
DIELECTRIC PLATES
a=10
θ=0°
Xo=1

FIG. 7b

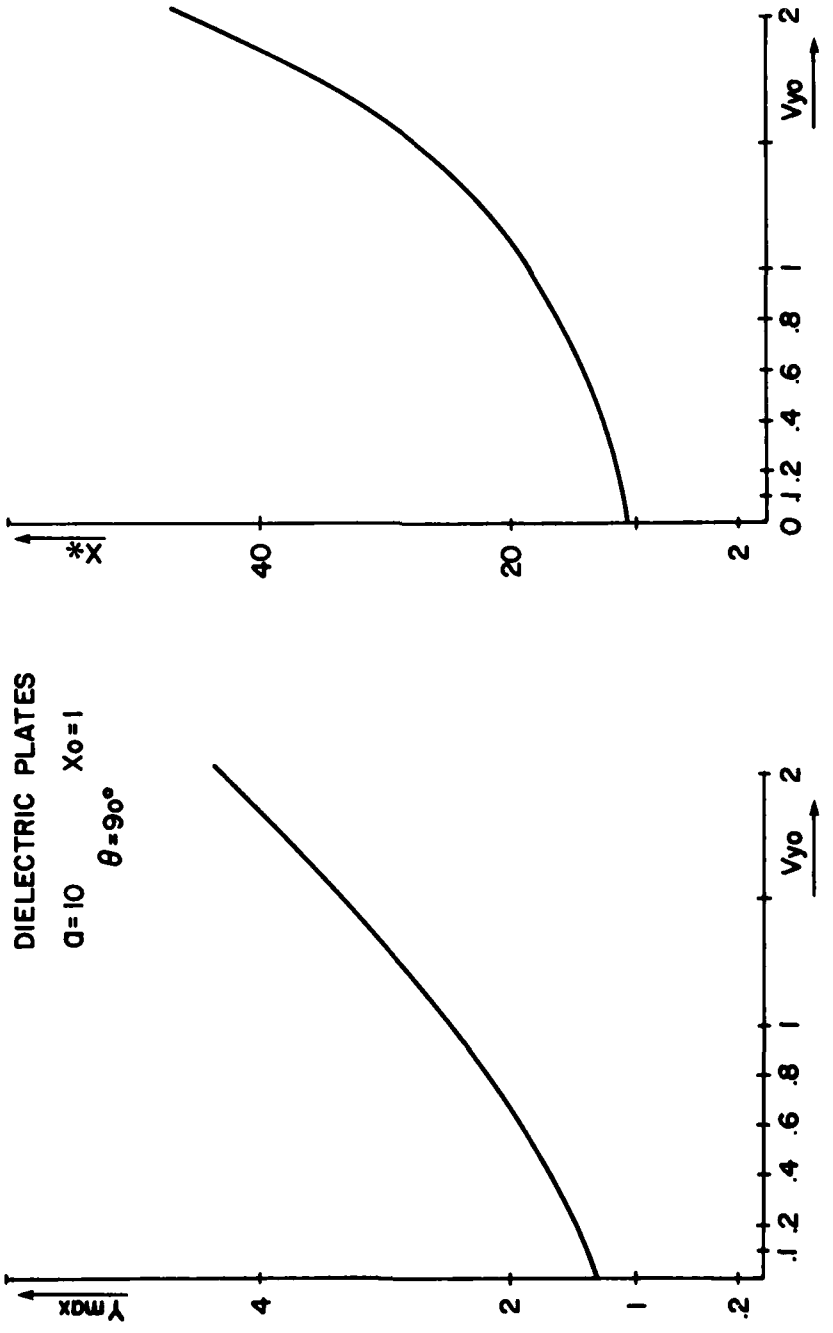
DIELECTRIC PLATES
a=10
Xo=1
θ=90°
γ MAX
.2
1
2
4
.1 .2 .4 .6 .8 1
Vyo
2
*X
2
20
40
0 .1 .2 .4 .6 .8 1
Vyo
2

FIG. 8

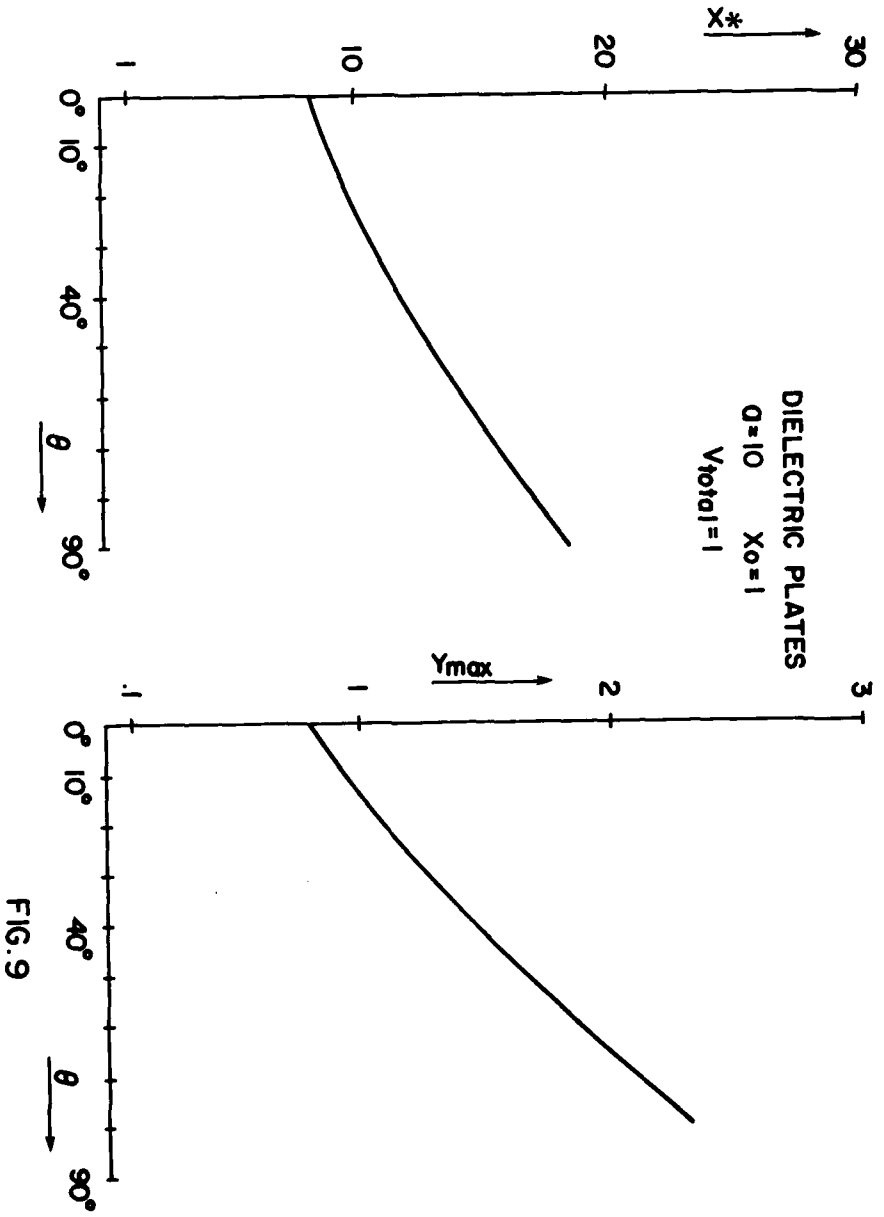
X*
30
20
10
1
0°
10°
40°
θ
90°
DIELECTRIC PLATES
a=10 Xo=1
Vtotal=1
Ymax
3
2
1
.1
0°
10°
40°
θ
90°

FIG.9

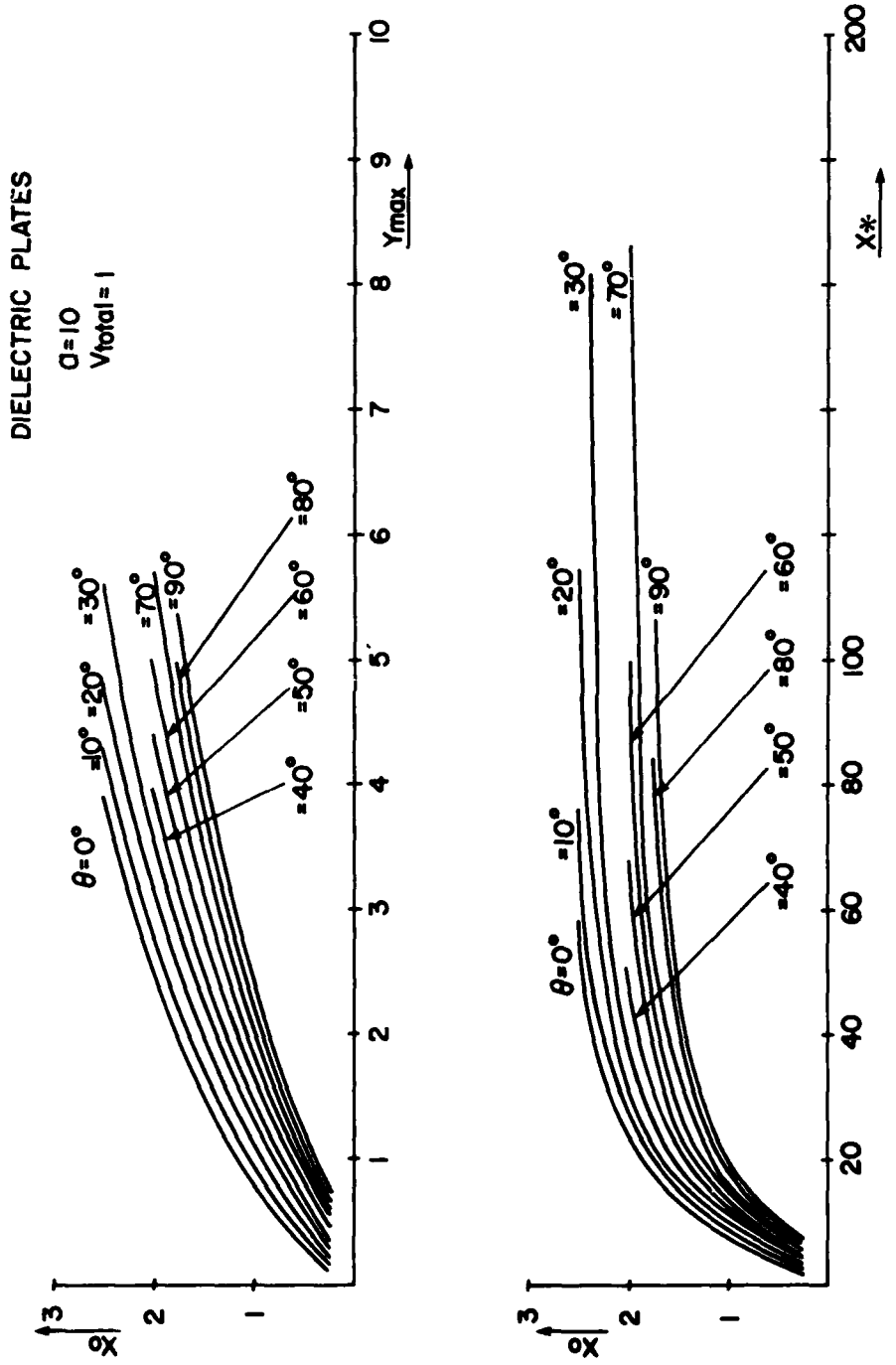
DIELECTRIC PLATES
a=10
Vtotal=1
θ=0°
=10°
=20°
=30°
=40°
=50°
=60°
=70°
=80°
=90°
Ymax
X*
ox

FIG. 10